

## ARTICLES

## Fluorescence Study of the Sol–Gel Process in Hybrid Precursors: Evidence of Concentration Fluctuations at the Local Scale

Daodao Hu,<sup>†</sup> Céline Croutxé-Barghorn,<sup>\*,‡</sup> Mathieu Feuillade,<sup>‡</sup> and Christiane Carré<sup>‡</sup>

School of Chemistry and Material Science, Shaanxi Normal University, Xi'an 710062, People's Republic of China, and Département de Photochimie Générale, Centre National de la Recherche Scientifique Unité Mixte de Recherche 7525, ENSCMu, 3, rue Alfred Werner 68093, Mulhouse Cedex, France

Received: January 12, 2005; In Final Form: June 23, 2005

Hybrid sol–gel materials have been prepared by hydrolytic polycondensation of an alkoxysilane. The sol–gel process of methacryloxypropyltrimethoxysilane (MAPTMS) has been followed by fluorescence spectroscopy with 2-naphthol as a probe. The experimental results showed that this photoprobe was dramatically sensitive to the microenvironment polarity. Spectroscopic studies revealed fluctuations of the maximum emission intensity and wavelength as a function of time. These fluctuations were attributed to the amphiphilic behavior of the hydrolyzed precursor. The maximum emission wavelength of the probe corresponding to its protonated form was higher than in pure water. All the results suggest that the presence of water molecules, tightly bonded to the polar head of the silanols, increased locally the sol polarity and induced a red-shifted emission. Fluorescence spectroscopy emphasized the reversibility of monomeric silanol aggregates and the changes in hydroxy group number of the silica network during the sol maturation. The behavior of this system upon shaking confirmed this statement.

## I. Introduction

It is well-known that the sol–gel process allows organic molecules to be incorporated in an inorganic matrix under mild conditions. Since hybrid materials offer a large range of applications, including devices for linear and nonlinear optics, luminescent solar concentrators, chemical and pH sensors, etc., different routes to prepare these materials were developed.<sup>1–3</sup> It is therefore not surprising that much effort has been devoted to understanding the sol–gel process, which consists of two main steps: during the first one, a high surface area microporous glass is formed at room temperature by sol formation, gelation, and gel desiccation. In a second step, a nonporous glass is obtained by annealing the porous glass at high temperature. Following the route from the precursor to the final xerogel (dry gel) is required since the properties of the final material are intimately linked to its structure. Investigations at the atomic scale as well as at the nano- and microscale are, thus, primordial. A wide variety of analytical techniques, such as X-ray and neutron diffraction and infrared, Raman, or NMR spectroscopies, are commonly used in this way.<sup>4</sup> Although most of them allow studying the bulk sol–gel material, they do not provide detailed information on microenvironments at the molecular scale. Electron spectroscopy and especially emission spectroscopy are sensitive methods to scrutinize the local environment of a specific probe molecule.<sup>5,6</sup> Fluorescence technique is a useful technique not only to follow the process of heterogeneous systems but also to offer important information for the design

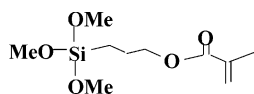
and synthesis of a wide range of novel materials, especially in the areas of photonics and chemical sensors.<sup>7,8</sup> Structural changes at the molecular scale of the inorganic backbone were studied for the first time by Avnir and Levy.<sup>9</sup> A probe with the suitable photophysical and photochemical properties was added to the system in order to monitor the sol–gel process of Si-(OMe)<sub>4</sub>. It allowed fundamental questions, such as the sol–gel chemistry or structural development during polymerization, gelation, and drying of gels, to be understood. It also provided information about the nature of interactions between guest dye molecules and the solid host matrix, or the parameters controlling the luminescence of molecules embedded in these inorganic systems. Rhodamine 6G,<sup>10</sup> pyrene,<sup>11</sup> pyranine,<sup>12</sup> and europium cation<sup>13</sup> have been widely used as photoprobes to monitor the sol–gel process. Because molecular mobility, solvation, and reorientation processes have a dominant effect in their electronic excited states, a given dye behaves differently in various solid matrices or sol–gel systems.<sup>14</sup>

Most of the previous papers focused on the sol–gel process of tetramethyl orthosilicate (TMOS),<sup>15</sup> tetraethyl orthosilicate (TEOS)<sup>16</sup> or mixed solutions of silicon and aluminum alkoxides.<sup>17</sup> No extensive study of hybrid precursors such as methacryloxypropyltrimethoxysilane (MAPTMS) has been performed as yet. Such organically substituted alkoxysilanes of the type (R'O)<sub>3</sub>Si–R, where R represents a functional group and R' a CH<sub>3</sub> or C<sub>2</sub>H<sub>5</sub> group, minimize the volume shrinkage resulting from the sol to xerogel transition and are an appropriate response to the current trends in optics.<sup>18</sup> In addition, alkoxysilanes, in which R is a polymerizable function, are extremely interesting for the synthesis of inorganic–organic glasses. In this approach, an organic network is formed in the

\* Corresponding author: e-mail c.barghorn@uha.fr; tel +33 3 89 33 68 35; fax +33 3 89 33 68 95.

<sup>†</sup> Shaanxi Normal University.

<sup>‡</sup> Département de Photochimie Générale, CNRS UMR 7525, ENSCMu.

**CHART 1: Chemical Structure of MAPTMS**

matrix of the primarily formed inorganic network. Polymerization is frequently carried out under thermal activation. However, to avoid thermal degradation of the organic molecules incorporated in the material for specific optical applications, a consolidation step under mild conditions is preferred. It corresponds to a photochemical process in which the organic groups are polymerized under UV or visible irradiation.

Recently, we reported on the effect of silicate backbone on the photopolymerization kinetics by means of real-time Fourier transform infrared and  $^{29}\text{Si}$  NMR spectroscopies.<sup>19,20</sup> The study mainly focused on the mechanisms of polymerization in hybrid sol–gel materials. Not much information was obtained on the hydrolysis and condensation dynamics of this hybrid precursor. However, the condensation state of the inorganic part of the molecule was found to affect the conversion ratio reached by the organic functions during the photopolymerization process.<sup>19</sup>

The present paper reports on the use of a photophysical probe, 2-naphthol, for investigating structural development and changes in the polar character of the surrounding species around the photoprobe molecule during the sol–gel process. Changes in the inorganic backbone structure of the hybrid precursor modify the amplitude of its interaction with the 2-naphthol that finally determine the probe location. Interestingly, because of the high sensitivity of the fluorescent probes to environmental factors in heterogeneous system, sol–gel systems lend themselves to this kind of investigation. The approach in the present study involves addition of a low concentration of probe, and the changes in the fluorescence properties resulting from changes in the probe environment were then monitored at the minute scale. The obtained results provided information on the sol conformation as hydrolysis and condensation reactions developed. They gave new insights into the sol–gel process in hybrid precursors and emphasized the influence of a long hydrophobic chain.

**II. Experimental Section**

**II.1. Chemicals.** Methacryloxypropyltrimethoxysilane (MAPTMS) was purchased from Aldrich. Its chemical structure is shown in Chart 1. Water was deionized. Methanol was spectroscopic-grade. Isooctane, hydrochloric acid, Triton X-100 (Wako Pure Chemicals Industries), and 2-naphthol (Aldrich) were reagent-grade.

**II.2. Sample Preparation.** Partial hydrolysis and condensation of MAPTMS were carried on by adding 0.75 molar equiv of acidified water (0.01 M HCl). Such experimental conditions correspond to a water/Si ratio ( $r_w$ ) of 0.75. 2-Naphthol at a concentration of  $1.7 \times 10^{-4}$  M was introduced just after the water addition. At the beginning of the reaction, water and MAPTMS were not miscible. As hydrolysis proceeded, methanol was gradually released in the mixture. The solution became clear after 4 min. Then the fluorescence measurements were performed at the minute scale. When used, Triton X-100 was added at a concentration of 0.086% (w/w).

**II.3. Instrumentation.** Optical absorption spectra of the solutions were recorded on a Beckman DU640 spectrophotometer and fluorescence spectra on a Fluoromax-2 (Jobin-Yvon) fluorescence spectrophotometer. Emission spectra were obtained with an excitation wavelength of 330 nm. The fluorescent cell was closed for all measurements.

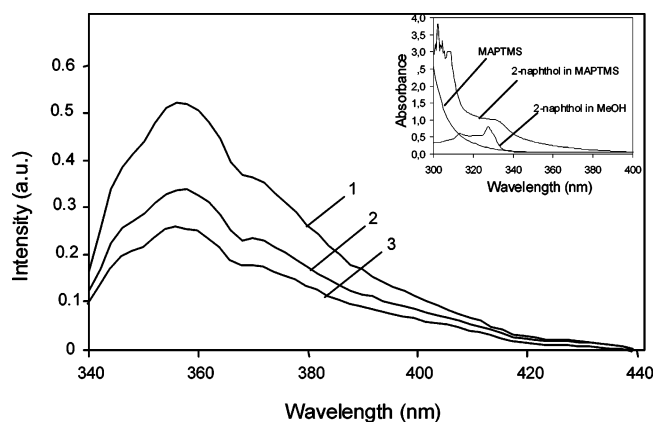


**Figure 1.** Fluorescence intensity decrease upon increasing 2-naphthol concentration in MAPTMS. Concentrations of 2-naphthol were  $1.7 \times 10^{-4}$ ,  $2.4 \times 10^{-4}$ , and  $3.4 \times 10^{-4}$  M in spectra 1, 2, and 3, respectively.

**III. Results and Discussion**

**III.1. Preliminary Study.** To understand the photophysical behavior of 2-naphthol during the sol–gel process, some preliminary experiments were carried out in standard solutions.

**III.1.1. Fluorescence Spectroscopy of 2-Naphthol in MAPTMS.** Figure 1 shows the fluorescence and absorption spectra of 2-naphthol (ArOH) in MAPTMS. The emission at 358 nm was assigned to the  $^*\text{ArOH}$  species. Despite the weak overlap between the excitation window centered at 330 nm and the absorption spectrum of the hybrid precursor, fluorescence of 2-naphthol is suited for investigating the sol–gel process.

Fluorescence spectra show a decrease in the emission intensity upon weakly increasing the 2-naphthol concentration (Figure 1). This observation was attributed to the aggregation of the probe molecules. Since 2-naphthol and MAPTMS are respectively dipolar and apolar molecules, the aggregation of 2-naphthol in MAPTMS can occur. This point will be developed in the following sections. With this phenomenon taken into account, a 2-naphthol concentration of  $1.7 \times 10^{-4}$  M was used throughout this work.

**III.1.2. Fluorescence Spectroscopy of 2-Naphthol in a Mixture of Methanol and Water.** It is a well-known fact that the acidity of 2-naphthol in aqueous solutions substantially increases upon photoexcitation.<sup>21</sup> In the  $S_1$  state, protolytic dissociation takes place in neutral aqueous solutions (pH = 5–7). The protonation of  $^*\text{ArO}^-$  (i.e.,  $^*\text{C}_{10}\text{H}_7\text{O}^-$ ) is much slower than deactivation of  $^*\text{ArO}^-$  and can be neglected. 2-Naphthol can, thus, be used to monitor the acid–base equilibrium process.

Since methanol and water are both byproducts of the hydrolysis and condensation reactions, fluorescence spectra of 2-naphthol were recorded in water (pH = 2)/methanol mixtures (Figure 2). Emission fluorescence intensity was recorded at 358 and 420 nm, which correspond to maximum emission of the  $^*\text{ArOH}$  and  $^*\text{ArO}^-$  species, respectively. The increase in fluorescence intensity at 358 nm was accounted for by the polarity decrease resulting from the addition of increasing amounts of methanol in water. It should be noticed that, even at low methanol concentration (high water content), the peak at 420 nm corresponding to the fluorescence of the excited deprotonated form was very weak. This result was attributed to the acidic conditions used in this study. Proton-transfer reactions took place and led to the back reaction corresponding to the protonation of  $^*\text{ArO}^-$ .

**III.1.3. Fluorescence Spectroscopy of 2-Naphthol in a Mixture of Methanol and MAPTMS.** Figure 3 shows the fluorescence spectra of 2-naphthol in the MAPTMS/methanol mixtures. Weak

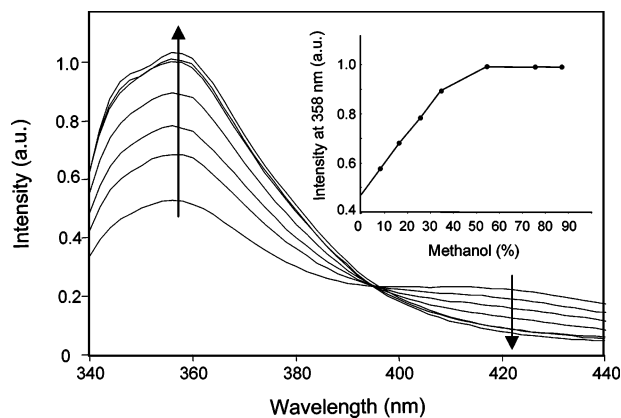


**Figure 2.** Fluorescence spectra of 2-naphthol ( $1.7 \times 10^{-4}$  M) in water (pH = 2)/methanol mixtures. (Inset) Corresponding changes in maximum emission intensity.

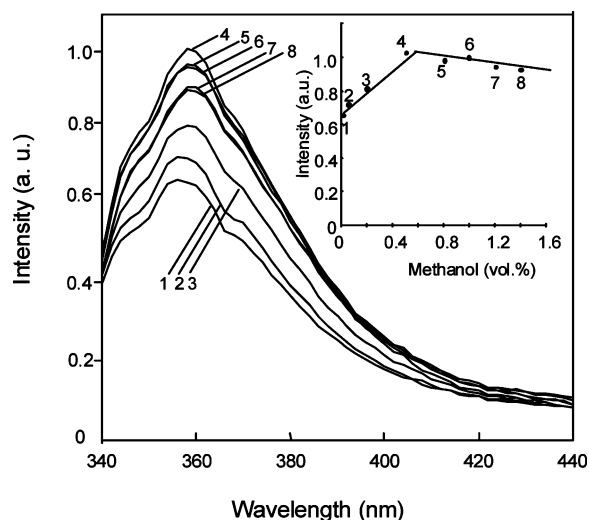


**Figure 3.** Fluorescence spectra of 2-naphthol ( $1.7 \times 10^{-4}$  M) in various MAPTMS/methanol mixtures (in volume percent).

increases in methanol concentration induced dramatic increases in fluorescence intensity. In addition, the maximum emission wavelength was red-shifted while a blue shift was expected,<sup>22</sup> thus suggesting that other factors have to be considered. It was visible from Figure 1 that the actual quantum yield of fluorescence was reduced in MAPTMS. The increase in intensity

observed in Figure 3 upon addition of methanol was attributed to the deaggregation of 2-naphthol.

A way to investigating the probe aggregation is UV spectroscopy. Indeed, changes in absorption spectra (either intensity or shape) due to the presence of new structures can provide information about the aggregation process. Unfortunately, there is an overlap between MAPTMS and 2-naphthol absorption spectra (Figure 1). To confirm the presence of dye aggregation, the same experiments were performed in isooctane (an apolar medium), instead of MAPTMS (Figure 4). When methanol concentration is increased, the maximum absorption wavelength is not continuously red-shifted (Figure 4a). A new peak at higher wavelength appears. In addition, an isosbestic point can be observed. It corresponds to the wavelength at which two species have the same absorptivity, such that if the sum of the concentrations of the compounds in solution is held constant, the absorbance at this point will be invariant as the ratio of the two compounds is varied. Existence of one or more such points is indicative of chemical equilibrium between the two compounds. The isosbestic point thus indicates that 2-naphthol is converted into another species. As a dipolar molecule, it forms aggregates in nonpolar solvent. We assigned the peaks at 327 and 331 nm to aggregates and the hydrogen-bonded complexes, respectively. Addition of methanol (Figure 4b) led to the formation of a complex with the 2-naphthol by hydrogen bonding. Photoprobe aggregation was thus reduced, resulting in an increase in emission intensity.

In light of this statement, it becomes possible to understand the unexpected behavior reported in Figure 3. Addition of methanol into MAPTMS led to an intensity increase due to the deaggregation of the probe molecules, and the red-shifted emission wavelength was obviously related to the polarity increase resulting thereof. The reason for the slight intensity decrease observed for methanol concentrations up to 0.6% should be related to the complexation of probe molecules through hydrogen bonding, which also quenches the fluorescence process. A similar phenomenon was already observed by Iwanek and Mattay.<sup>23</sup>

From a general viewpoint, the experimental results reported in this section corroborate the fact that aggregation processes account for concentration quenching of the probe luminescence.<sup>24</sup>

**III.1.4. Conclusion.** The results reported in this preliminary study clearly substantiate the sensitivity of the naphthol probe

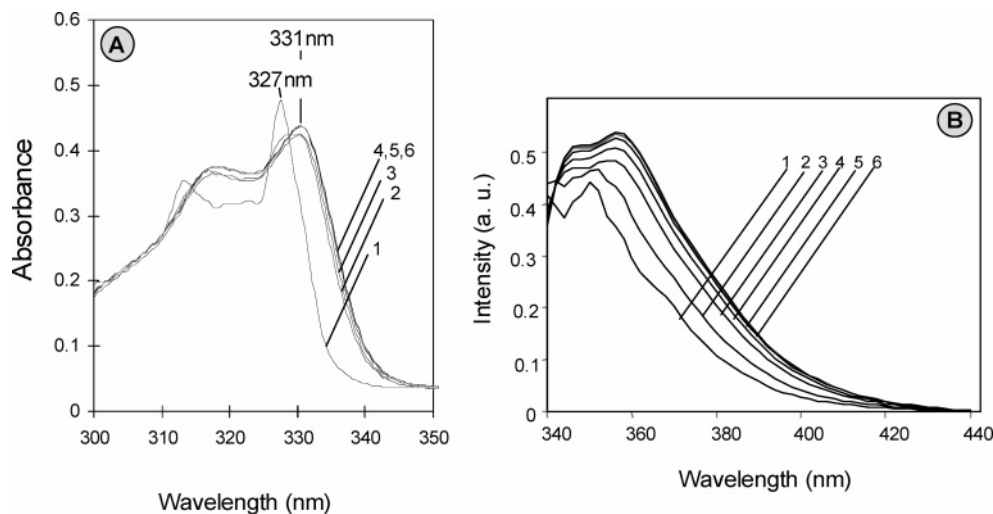


**Figure 4.** Optical absorption (A) and fluorescence (B) spectra of 2-naphthol ( $1.7 \times 10^{-4}$  M) in isooctane/methanol mixtures. Concentrations of MeOH (in volume percent) were 0, 0.3, 0.6, 1, 1.3, and 1.6 for spectra 1–6, respectively.

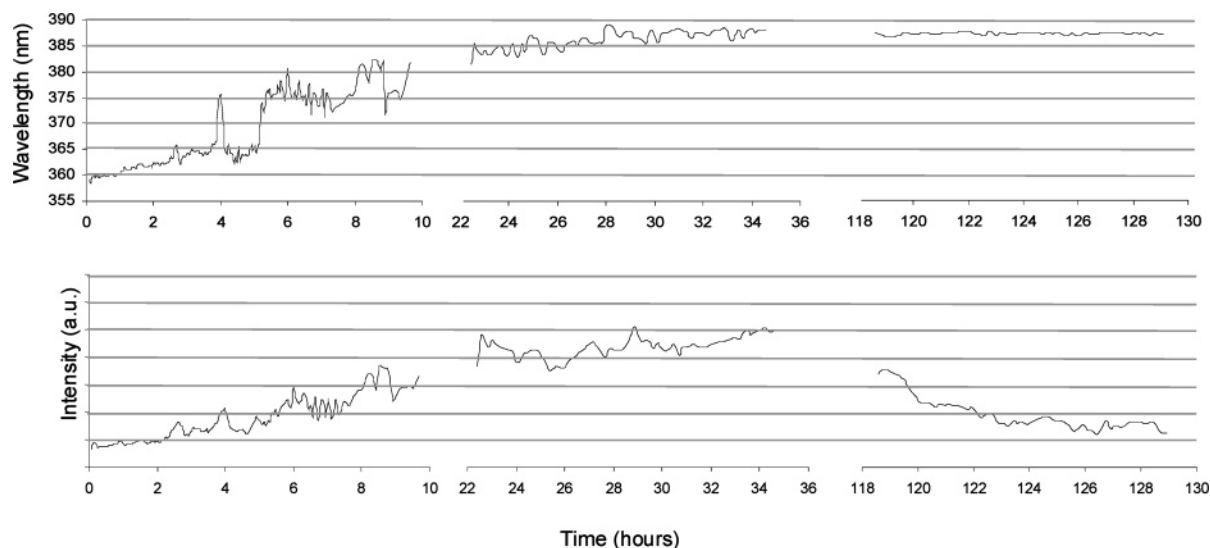


**Figure 5.** Evolution of emission wavelength at maximum and emission intensity of 2-naphthol as a function of maturation time.

to its surrounding. The emission intensity and wavelength at maximum increase with the polarity of the environment. Fluorescence intensity of 2-naphthol is strongly inhibited in MAPTMS. Aggregation of 2-naphthol in MAPTMS—respectively dipolar and apolar molecules—accounts for this behavior. Deaggregation of the probe occurs upon addition of methanol to the nonhydrolyzed hybrid precursor. It shows itself in an increased and red-shifted emission. The fluorescence yield of the excited deprotonated form ( $^*ArO^-$ ) was observed to be very weak, a feature attributed to the acidic conditions used in this preliminary study. It is worth noting that such acidic conditions are prevailing in the initiating step of the sol–gel condensation process.

### III.2. Fluorescence Study of the Sol–Gel Process: III.2.1.

**General Comments.** Figure 5 shows two sets of three graphics corresponding to the fluctuations in emission wavelength at maximum and emission intensity of 2-naphthol in a sol–gel formulation as a function of time. The system does not reach equilibrium but reveals a fluctuating character. Both parameters (wavelength and intensity) seem to behave identically to some extent. Great care was taken to establish the authenticity of this unexpected behavior. Interestingly, the results can be reproduced and the amplitude of the fluctuation observed depends on experimental conditions (amount of water, pH, etc.). As will be explained below, these observations were attributed to local changes in probe concentration. The following sections of this paper will concentrate on a thorough study of each of the stages reported in Figure 5.

**III.2.2. From 0 to 5 Hours.** As shown in the preliminary study, changes in local dye concentration can account for variations in emission intensity and maximum emission wavelength. The fluctuations observed in Figure 5 indicate that the environment strongly influences the fluorescence of 2-naphthol. Conversely, the fluorescence spectra reflect changes in chemical species surrounding the probe.

At the beginning of the sol–gel process (up to 5 h), hydrolysis reactions produce methanol and silanol species. The hybrid precursor becomes an amphiphilic molecule with a polar head and an apolar tail corresponding to the nonhydrolyzable organic moiety. The sol can thus, be compared to a surfactantlike structure. 2-Naphthol is a dipolar molecule. At the beginning of the hydrolysis process, it is located near the organic part of MAPTMS. As hydrolysis proceeds, 2-naphthol and water molecules can interact with silanol functions through hydrogen

bonding. Probe aggregation in the bulk phase is therefore reduced and the fluorescence intensity increases. In addition, the polarity of the immediate vicinity of the probe molecules increases, thus leading to a red-shifted emission. Methanol is the byproduct of hydrolysis and condensation reactions. It is soluble in both apolar and polar environments. Increasing methanol amounts in the reactive medium can destroy the surfactant conformation. 2-Naphthol molecules are thus released by the silanols to the bulk phase. As a result, the fluorescence intensity decreases dramatically and the wavelength is blue-shifted. It becomes thus easy to understand that the methanol/silanols ratio is the key factor accounting for the fluctuations. The amphiphilic property of MAPTMS accounts for the fluctuations, which are closely related to the reversible aggregation of silanols during the first hours of the sol–gel process. Such behavior was not observed when 2-naphthol was used as a probe to monitor the sol–gel process of TEOS (tetraethyl orthosilicate).<sup>16</sup> This precursor does not exhibit an amphiphilic character.

The emission wavelength at maximum of the protonated form of 2-naphthol shifts up to 375 nm. Figure 2 showed that it did not exceed 360 nm even in pure water. This wavelength increase must be attributed to the probe environment in the surfactantlike structure, which is more polar than in bulk phase. It has been shown elsewhere that hydrogen bonding between the probe and silanol groups is particularly important in restricting the molecular motions.<sup>25</sup> The behavior of water molecules in a confined environment such as surfactant structure is different from that in the bulk phase. The basicity is lowered owing to tight binding to silicate groups. This effect induces both a polarity increase and a lowering of the proton acceptance.<sup>26</sup> Recently, similar fluorescence behavior of 2-naphthol derivatives in Langmuir–Blodgett films has been reported by Mironczyk et al.<sup>27</sup> Such restriction of mobility due to hydrogen bonding was also reported to induce drastic changes in thermodynamic, structural, and dynamic properties of embedded molecules.<sup>28,29</sup>

The gradual wavelength increase during the first 5 h is thus attributed to the polarity increase of the bulk phase, due to methanol production by the hydrolysis.

**III.2.3. From 6 to 36 Hours.** The behavior of the sol–gel system seems to change after a 5-h maturation period. A dramatic increase in the emission wavelength at maximum is observed, and it finally levels at ca. 387 nm. To understand this result, characterization of the sol was also achieved by liquid-state <sup>29</sup>Si NMR spectrometry. The spectrum of a sol after



X = CH<sub>3</sub> or H  
R = organic functional group

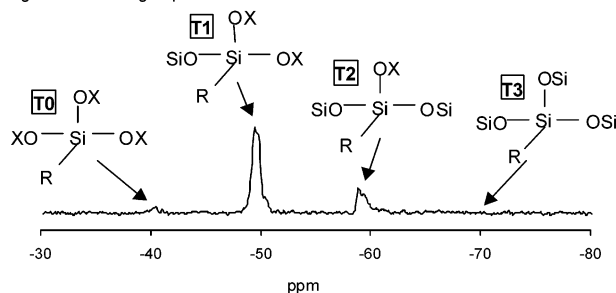


**Figure 6.** Liquid <sup>29</sup>Si NMR spectrum of the MAPTMS sol after 5 h of maturation.

a 5-h maturation period is presented in Figure 6. T0 species correspond to free precursor molecules. T1 signal (−49 to −51 ppm) is related to terminal Si atoms at the end of a silicate chain. T2 and T3 species refer to Si atom linked to two and three O–Si functions, respectively.

It can be seen from Figure 6 that almost no T0 species are visible at −41 ppm. This result indicates that no more free precursor molecules are present in the sol. No T3 species are visible in the NMR spectrum of 5-h matured sols. This result is not surprising since the precursor is not very reactive and acid conditions favor linear condensation chains rather than crosslinking.<sup>18</sup> The sol–gel system mainly consists of linear chains. It is possible to estimate the degree of condensation (DC) of the sol. DC is defined as  $\sum_n nT_t^n/f$ , where  $f$  is the maximum connectivity for a precursor (for MAPTMS  $f = 3$ ),  $n$  is the connectivity of the silicon site ( $1 \leq n \leq 3$ ), and  $T_t^n$  represents the total concentration of all species with the connectivity  $n$  (e.g.,  $T_t^1 = T1_{(0)} + T1_{(1)} + T1_{(2)}$ , where the  $t$  notation corresponds to the number of hydroxy groups).<sup>30</sup> In the case of a random polymerization of the trialkoxysilanes, gelation would occur at  $\alpha_c = 0.5$ , according to the relation  $\alpha_c = 1/(f - 1)$ , where  $\alpha_c$  is the critical conversion at the gel point. In acidic conditions, it has been shown that trialkoxysilanes may have important amounts of cyclic species present, so that the gel point is shifted to higher conversion degrees or the gelation can even not happen.<sup>31</sup> As reported by Loy et al., gelation also highly depends on the nature of the organic moiety.<sup>32</sup> According to the experimental conditions used in this study, the gelation was not observed in the prepared sols for  $r_w \leq 3$  even for high DC.

When fluorescence and NMR experiments are paralleled, one can conclude that the sharp increase in emission wavelength must be attributed to the fact that the SiOSi linear chain structure becomes predominant after 5 h. An irreversible adsorption of the photoprobe molecules by the inorganic network occurs, and the emission wavelength keeps up at the highest values. Furthermore, at low water/Si ratios ( $r_w \ll 2$ ), the condensation mechanism producing methanol is favored.<sup>33</sup> In consequence, condensation reactions do not go hand in hand with a strong decrease in hydroxy groups. The polarity of silicate groups remains high; hence the high value of the emission wavelength at maximum. The fluctuations observed after a 5-h maturation period result in structural changes of the inorganic oligomers due to further hydrolysis and condensation of methoxy and silanol groups.

To corroborate the assumption that the sharp wavelength increase is linked to the disappearance of the free precursor, experiments were carried out with higher amounts of water. Figure 7 shows a comparison between the fluctuations in emission wavelength at maximum for two water/Si ratios ( $r_w = 0.75$  and  $r_w = 3$ ).

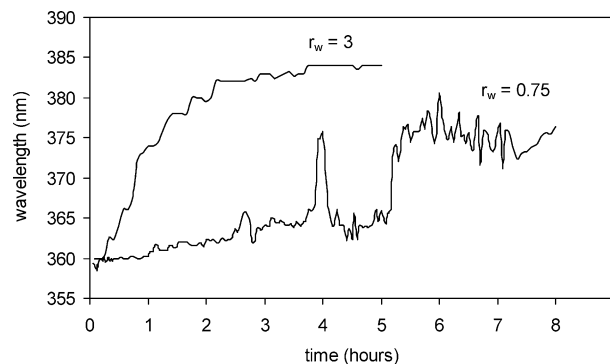


**Figure 7.** Influence of water/Si ratio on evolution of the emission wavelength at maximum of 2-naphthol as a function of time.

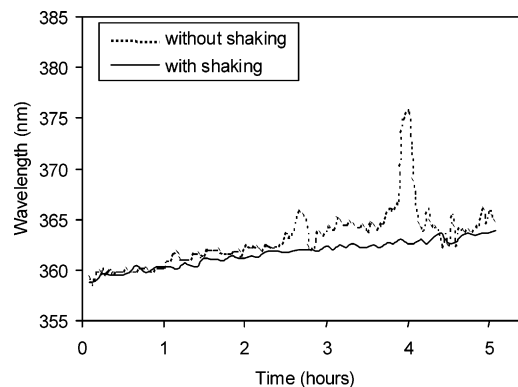


**Figure 8.** Influence of stirring the sample prior to measurement on fluctuations of the emission wavelength at maximum.

It is well-known that the major consequence of an increase in  $r_w$  is the acceleration of the hydrolysis reaction.<sup>18</sup> In addition, a thorough hydrolysis of methoxy groups takes place before significant condensation occurs. Condensation is also enhanced at higher  $r_w$  ratios, and water-forming reactions are favored.<sup>33</sup> Taking these differences into account allows the fluorescence behavior of systems with  $r_w = 3$  to be understood. Due to the acceleration of hydrolysis, the free precursor concentration sharply decreases, which favors the formation of Si–O–Si oligomers. Almost no fluctuation is observed. This result is attributed to more important amounts of methanol that keep silanols from aggregating. Oligomer structures exhibit a strong propensity to adsorb probe and water molecules. The presence of hydroxy groups resulting from hydrolysis of the methoxy groups increases the local polarity of 2-naphthol surroundings and leads to an increase in emission wavelength at maximum. The slight changes in emission wavelength only reflect further condensation in silicate oligomers. This observation clearly indicates that addition of increasing amounts of water accelerates not only the hydrolysis but also the condensation degree.

To confirm the existence of a time-dependent heterogeneity of the probe concentration related to silanol aggregates that are generated as the sol–gel maturation proceeds, the sol–gel process was followed up with samples shaken prior to measurement. The results of this experiment are reported in Figure 8. Fluctuations of the emission wavelength at maximum were dramatically reduced. Shaking the sample leads to a more homogeneous system in which the probe is uniformly distributed.

Between 22 and 36 h, the fluctuations in emission intensity and wavelength smooth down. The wavelengths fluctuate within a few nanometers around 385 nm, indicating that condensation is the major reaction. The probe locates in the more polar region, that is, the growing inorganic oligomers. Contrary to silanol

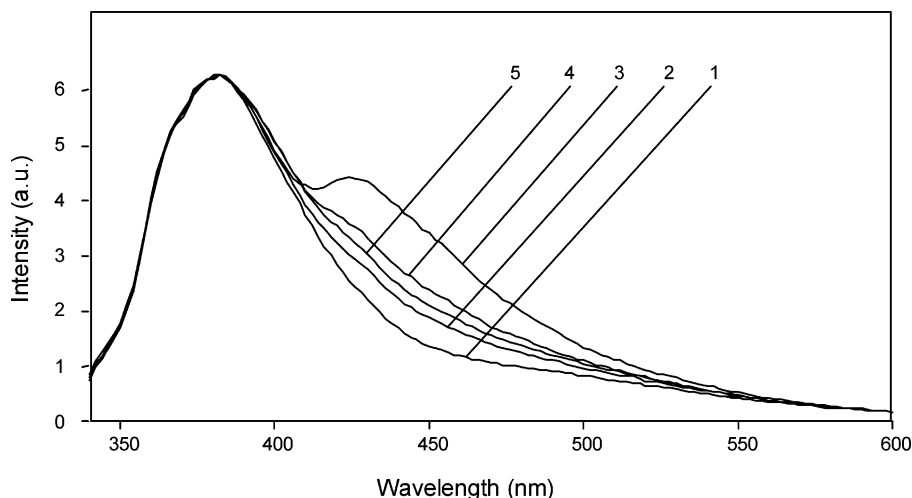


**Figure 9.** Normalized fluorescence spectra of 2-naphthol for long maturation times: (1) 125, (2) 135, (3) 153, (4) 275, and (5) 325 h.

aggregates, silicate oligomers enhance the irreversible adsorption of the probe molecules and water. Thus, the polarity around 2-naphthol remains high and the slight fluctuations in emission intensity and wavelength reflect weak polarity changes resulting from fluctuations in the hydroxy group number. Hydrolysis and condensation reactions proceed further during this stage and result in linear silicates oligomers or three-membered cyclic species. No T3 species can be distinguished. Even a higher water-to-silicone ratio ( $r_w = 1.5$ ) did not lead to the formation of branched structures (T3 species). NMR investigations showed that T2 species are predominant after 24 h of maturation.

**III.2.4. Long Maturation times (>100 Hours).** Changes in emission wavelength and intensity have to be correlated to changes in the sol structure. During this period, the silica network gradually extends, entrapping 2-naphthol and water molecules near the polar sites. The maximum emission wavelength is thus red-shifted and the fluorescence intensity decreases. Selected normalized fluorescence emission spectra corresponding to long maturation times ( $t > 125$  h) are presented in Figure 9.

A weak fluorescence increase is visible in the region where  $^*ArO^-$  species are known to absorb (ca. 420 nm). It is assigned to the presence of bulk water around the probe. Depending on the structure of silica network, the probe molecules partition between two microphases: in the first one, water molecules are tightly bound to the polar heads of the inorganic backbone. Depending on the extent of the condensation process, the probe molecules experience environments with various polarities. From the beginning up to 135 h, water molecules are strongly interacting with the silanol groups. The emission of 2-naphthol dissolved therein is centered at ca. 390 nm. In the next stage of the process, due to the progress of the condensation and the depletion of SiOH groups, the average distance between water molecules and silanol groups increases. The emission of some of the probe molecules dissolved in free water, in all respects identical to bulk water, shifts to ca. 420 nm. This emission wavelength is the typical signature of  $^*ArO^-$  species in pure water. In the last stage of the condensation process, due to the low  $r_w$  value, water molecules disappear completely. Then the probe fluorescence undergoes a blue shift back to what was observed in MAPTMS/methanol systems. Similar behavior was already reported in reverse micellar aggregates of hexadecyltrimethylammonium or sodium 1,4-bis(2-ethyl-hexyl)sulfosuccinate in  $CHCl_3$  when investigated by fluorescence techniques with pyranine (PyOH) as a probe.<sup>34</sup>

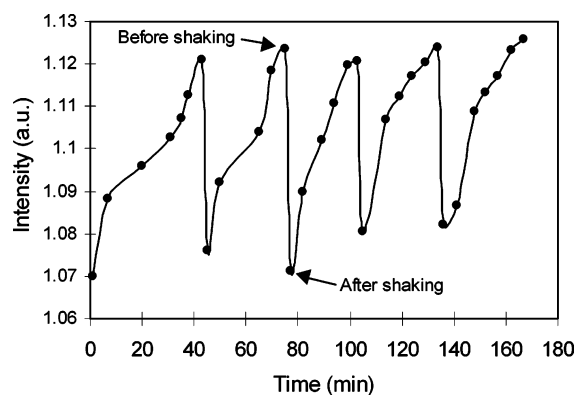


**Figure 10.** Influence of intermittent shaking on the fluorescence intensity fluctuations. After the sol was shaken, fluorescence spectra were recorded every minute over a period of 20–40 min.

To corroborate the assumption of entrapped probe molecules into the silica network, the influence of shaking was studied on a sol aged for 3 weeks (Figure 10). It has to be mentioned that at the low  $r_w$  used in this study the gel point was not reached even for a 3-week aged sol, which exhibits a viscosity of ca. 100 mPa·s. After the sol was shaken, fluorescence spectra were recorded every minute over a period of 20–40 min. Then the solution was shaken again and this procedure was repeated five times.

Immediately after shaking, the maximum emission intensity decreases dramatically and the wavelength is sharply blue-shifted. Then the intensity increases and the wavelength red-shifts back to its initial value. This result confirms that the probe molecules, which have a tendency to spontaneously become entrapped in the polar inorganic network, are redistributed by shaking. 2-Naphthol desorbs from the highly polar silica network and distributes homogeneously in the bulk phase with lower polarity. Then the inorganic network gradually readsorbs the probe molecules and returns to its initial state. It has to be noticed that this reversible phenomenon is different from the so-called “bottleneck effect” that was reported in the case of dry gels. In this case, host molecules are irreversibly entrapped by the network.<sup>35,36</sup>

#### IV. Conclusion

A hybrid sol–gel material was prepared by hydrolysis and condensation of an organic–inorganic precursor (MAPTMS). The time development of the sol–gel process was followed by

use of 2-naphthol as a fluorescent probe. It was established that this probe was sensitive to internal solvent chemistry and structural conformation of the silicates. Since the nature of the hybrid precursor leads to an inhomogeneous sol, the results presented in this study differ from those relating to precursors with lower molecular weights, such as Si(OMe)<sub>4</sub>. Fluorescence spectroscopy reveals that the system does not reach equilibrium. A fluctuation in the emission characteristics—both intensity and wavelength—was observed at the minute scale. The results give new insights in the sol–gel process and emphasize the influence of a long hydrophobic chain in the hybrid precursor. Hydrolyzed MAPTMS based on silanol functions with a long organic chain can be compared to a surfactant. The fluctuations in 2-naphthol fluorescence reflect changes in location resulting from a variable degree of aggregation of the silanol groups. As condensation proceeds, the branched silica structure extends and accounts for the irreversible adsorption of the probe molecules in the more polar region of the system.

For the first time, this paper emphasizes changes at a minute scale of the environment of a polarity-sensitive fluorescent molecule during a sol–gel process. It stresses the importance of an appropriate choice of such a photoprobe for monitoring the sol–gel process of hybrid precursors because of the coexistence of nanodomains and bulk phase with highly different local polarities and possible specific interactions of the probe.

## References and Notes

- (1) Hench, L. L.; West, J. K. *Chem. Rev.* **1990**, *90*, 33.
- (2) Prasad, P. N.; Williams, D. J. *Introduction to non linear optical effect in molecules and polymers*; Wiley: New York, 1991.
- (3) Kuselmen, I.; Lev, O. *Talanta* **1993**, *40*, 749.
- (4) Almeida, R. M.; Sakka, S. *Handbook of Sol–Gel Science and Technology*, Vol. II; Kluwer Academic Publishers: Boston, MA, 2005.
- (5) Beddard, G. S.; West, M. A. *Fluorescent Probes*; Academic Press: New York, 1981.
- (6) Dunn, B.; Zink, J. I. *J. Mater. Chem.* **1991**, *1*, 903.
- (7) Sakka, S. *Handbook of Sol–Gel Science and Technology*, Vol. III; Kluwer Academic Publishers: Boston, MA, 2005.
- (8) Klein, L. C. *Sol Gel Optics, Processing and Applications*; Kluwer Academic Publishers: Boston, MA, 1994.
- (9) Avnir, D.; Levy, D. R. *J. Phys. Chem.* **1984**, *88*, 5956.
- (10) Innocenzi, P.; Kozuka, H.; Yoko, T. *J. Non-Cryst. Solids* **1996**, *201*, 26–36.
- (11) Chambers, R. C.; Haruvy, Y.; Fox, M. A. *Chem. Mater.* **1994**, *6*, 1351.
- (12) Pouxviel, J. C.; Dunn, B.; Zink, J. I. *J. Phys. Chem.* **1989**, *93*, 2134.
- (13) Levy, D. R.; Avnir, D. *Chem. Phys. Lett.* **1984**, *109*, 593.
- (14) Matsui, K.; Tomonaga, M.; Arai, Y.; Saton, H.; Kyoto, M. *J. Non-Cryst. Solids* **1994**, *169*, 295.
- (15) Kaufman, V. R.; Avnir, D. *Langmuir* **1986**, *2*, 717.
- (16) Fujii, T.; Mabuchi, T.; Mitsui, I. *Chem. Phys. Lett.* **1990**, *168*, 5.
- (17) Fujii, T.; Mabuchi, T.; Kitamura, H.; Kawauchi, O.; Negishi, N.; Anpo, M. *Bull. Chem. Soc. Jpn.* **1992**, *65*, 720.
- (18) Brinker, C. J.; Scherer, G. W. *Sol–Gel Science: The Physics and Chemistry of Sol–Gel Processing*; Academic Press: San Diego, 1990.
- (19) Soppera, O.; Croutxé-Barghorn, C. *J. Polym. Sci., Part A: Polym. Chem.* **2003**, *41*, 716.
- (20) Soppera, O.; Croutxé-Barghorn, C. *J. Polym. Sci., Part A: Polym. Chem.* **2003**, *41*, 831.
- (21) Il'ichev, Y. V.; Demyashkevich, A. B.; Kuzmin, M. G. *J. Photochem. Photobiol., A: Chem.* **1993**, *74*, 51.
- (22) Suppan, P.; Ghoneim, N. *Solvatochromism*; The Royal Society of Chemistry: Cambridge, U.K., 1997.
- (23) Iwanek, W.; Mattay, J. *J. Photochem. Photobiol., A: Chem.* **1992**, *67*, 209.
- (24) Veshin, V. L. *Z. Phys.* **1927**, *43*, 230.
- (25) Nikiel, L.; Hopkins, B.; Zerda, T. W. *J. Phys. Chem.* **1990**, *94*, 7458.
- (26) Sunamoto, J.; Hamada, T. *Bull. Chem. Soc. Jpn.* **1978**, *51*, 3130.
- (27) Mironczyk, A.; Jankowski, A.; Chyla, A.; Ozyhar, A.; Dobryszewski, P. *J. Phys. Chem. A* **2004**, *108*, 5308.
- (28) Brodka, A.; Zerda, T. W. *J. Chem. Phys.* **1992**, *97*, 5669.
- (29) McKierian, J.; Simomi, E.; Dunn, B.; Zink, J. I. *J. Phys. Chem.* **1994**, *98*, 1006.
- (30) Dong, H.; Lee, M.; Thomas, R. D.; Zhang, Z.; Reidy, R. F.; Mueller, D. W. *J. Sol-Gel Sci. Technol.* **2003**, *28*, 5.
- (31) Devreux, F.; Boilot, J. P.; Chaput, F.; Lecomte, A. *Phys. Rev. A* **1990**, *41*, 6901.
- (32) Loy, D. A.; Baugher, B. M.; Baugher, C. R.; Schneider, D. A.; Rahimian, K. *Chem. Mater.* **2000**, *12*, 3624.
- (33) Assink, R. A.; Kay, B. D. *J. Non-Cryst. Solids* **1988**, *99*, 359.
- (34) Kondo, H.; Miwa, I.; Sunamoto, J. *J. Phys. Chem.* **1982**, *86*, 4826.
- (35) Parad, N. P.; Bright, F. V. *J. Phys. Chem.* **1994**, *98*, 17.
- (36) Fujii, T.; Mabuchi, T.; Mitsui, I. *Chem. Phys. Lett.* **1990**, *168*, 5.